Available online at www.sciencedirect.com
ScienceDirect
Journal of Power Sources 178 (2008) 699–705
JOURNAL OF POWER SOURCES
www.elsevier.com/locate/jpowsour

Impacts of air bleeding on membrane degradation in polymer electrolyte fuel cells

Minoru Inaba *, Masashi Sugishita, Junpei Wada, Koichi Matsuzawa, Hirohisa Yamada, Akimasa Tasaka

Department of Molecular Science and Technology, Faculty of Engineering, Doshisha University, Kyotanabe, Kyoto 610-0321, Japan

Received 15 July 2007; received in revised form 20 August 2007; accepted 20 August 2007
Available online 24 August 2007

Abstract

A long-term accelerated test (4600 h) of a 25 cm^2 single cell with excess air bleeding (5%) was carried out to investigate the effects of air bleeding on membrane degradation in polymer electrolyte fuel cells. The rate of membrane degradation was negligibly low (fluoride-ion release rate = 1.3×10^{-10} mol cm^{-2} h^{-1} in average) up to 2000 h. However, membrane degradation rate was gradually increased after 2000 h. The CO tolerance of the anode gradually dropped, which indicated that the anode catalyst was deteriorated during the test. The results of the rotating ring–disk electrode measurements revealed that deterioration of Pt–Ru/C catalyst by potential cycling greatly enhances H_2O_2 formation in oxygen reduction reaction in the anode potential range (~0 V). Furthermore, membrane degradation rate of the MEA increased after the anode catalyst was forced to be deteriorated by potential cycling. It was concluded that excess air bleeding deteriorated the anode catalyst, which greatly enhanced H_2O_2 formation upon air bleeding and resulted in the increased membrane degradation rate after 2000 h.

Keywords: Polymer electrolyte fuel cells; Pt–Ru/C anode catalyst; Air bleeding; Membrane degradation; Hydrogen peroxide

1. Introduction

Durability is one of the most important issues in commercialization of polymer electrolyte fuel cells (PEFCs). Unfortunately, sufficient durability of PEFC cell stacks has not been established yet. One of the serious problems is the deterioration of perfluorinated sulfonic acid (PFSA) membrane used as an electrolyte [1–10]. It is now widely recognized that the formation of hydrogen peroxide, which is formed upon catalytic combustion of hydrogen with crossover oxygen at the anode catalyst layer [5,7–9] or at the Pt band formed in the vicinity of the cathode catalyst layer inside the membrane [7,10], plays an important role in membrane degradation under open-circuit conditions:

$$H_2 + Pt \rightarrow Pt\text{–}H \text{ (at anode)} \quad (1)$$

$$Pt\text{–}H + O_2 \text{ (diffused through PEM to anode)} \rightarrow {}^{\bullet}OOH \quad (2)$$

$$^{\bullet}OOH + Pt\text{–}H \rightarrow H_2O_2 \quad (3)$$

Furthermore, reactive oxygen radicals ($^{\bullet}OH$ and $^{\bullet}OOH$) are formed from hydrogen peroxide in the presence of minor impurities such as Fe^{2+} and Cu^{2+} ions:

$$H_2O_2 + M^{2+} \text{ (found in MEA)} \rightarrow M^{3+} + {}^{\bullet}OH + OH^- \quad (4)$$

$$^{\bullet}OH + H_2O_2 \rightarrow H_2O + {}^{\bullet}OOH \quad (5)$$

which greatly accelerates membrane degradation [6,8].

In PEFC-based stationary co-generation systems, which are intensively developed in Japan, Pt–Ru/C catalyst is used as an anode because reformed gas contains a small amount of CO. It has been recently reported that the CO tolerance of the Pt–Ru/C catalyst deteriorates gradually in long-term operation, which leads to a significant drop in voltage [11,12]. It is widely known that air bleeding is very effective to compensate the drop in CO tolerance of the anode [13,14]. However, introduction of a small amount of oxygen into the hydrogen atmosphere at the anode produces a large amount of H_2O_2 according to Eqs. (1)–(3) and may cause serious membrane degradation in long-term operation with air bleeding. In the present study, a long-term acceler-

* Corresponding author. Tel.: +81 774 65 6591; fax: +81 774 65 6841.
E-mail address: minaba@mail.doshisha.ac.jp (M. Inaba).

0378-7753/$ – see front matter © 2007 Elsevier B.V. All rights reserved.
doi:10.1016/j.jpowsour.2007.08.040

Nomenclature

FRR	fluoride-ion release rate in drain water (mol cm^{-2} h^{-1})
GC	glassy carbon
GDL	gas diffusion layer
I_D	disk current (A)
I_R	ring current (A)
IC	ion chromatograph
MEA	membrane-electrode assembly
N	collection efficiency for RRDE
N_{th}	theoretical collection efficiency for RRDE
ORR	oxygen reduction reaction
PEFC	polymer electrolyte fuel cell
PFSA	perfluorinated sulfonic acid
Pt/C	platinum catalyst supported on carbon
Pt–Ru/C	platinum–ruthenium alloy catalyst supported on carbon
RHE	reversible hydrogen electrode
RRDE	rotating ring–disk electrode
U_f	utilization of fuel (%)
U_o	utilization of oxygen (%)
$X_{H_2O_2}$	H_2O_2 yield in ORR (%)

ated test with an excess amount of air bleeding was carried out, and the impacts of air bleeding on membrane degradation were investigated.

2. Experimental

2.1. PEFC single cell

The membrane-electrode assemblies (MEAs) were of standard specifications designed for use in 1 kW class stationary PEFC co-generation systems using reformed gas as a fuel, and were manufactured in 2005 [7]. They consisted of PFSA membrane, Pt–Ru/C anode, Pt/C cathode, and gas diffusion layers (GDLs). The thickness of the membrane was 30 μm. The geometric surface area of both electrodes was 25 cm^2, and the catalyst loadings were 0.45 and 0.40 mg_{metal} cm^{-2} for the anode and cathode, respectively. Carbon paper and carbon cloth were used as GDLs for the anode and cathode, respectively. The MEA was pressed between two graphite separators with co-flow serpentine gas channels to make a single cell.

2.2. Accelerated air-bleeding test

An accelerated air-bleeding test was carried out at a cell temperature of 70 °C and at a current density of 200 mA cm^{-2} under highly humidified conditions, using a fuel cell testing system (Chino Corp., FC5100) equipped with an electrical load. Hydrogen gas (99.999%) from a hydrogen generator (Round Science, RHG-100) was mixed with 1000 ppm CO (H_2 balance, Taiyo Nissan) and filtered air to make a fuel gas (H_2 + 10 ppm CO + 5% air in volume). The fuel gas was humidified at 67 °C and fed to the anode (U_f = 40%) at ambient back-pressure, while filtered air was humidified at 67 °C, and fed to the cathode (U_o = 40%). Prior to the durability test, the cell was aged without air bleeding for 1 week using a pure hydrogen fuel and air.

Hydrogen crossover across the membrane was evaluated every 100 or 200 h during the accelerated test by an electrochemical method described elsewhere [5,7]. Pure hydrogen and argon (Taiyo Nissan, 99.9999%) was fed to the anode and the cathode, respectively, at 300 mL min^{-1} each. The potential of the cathode (in Ar) was swept at 1 mV s^{-1} from the rest potential (100–120 mV) to 500 mV against the anode (H_2/H^+). Hydrogen crossover was evaluated in diffusion-limited hydrogen oxidation current density obtained in the range of 300–350 mV.

The drain water from the cathode and anode was collected separately, and fluoride ions, which are decomposition products of the PFSA membrane, eluted in the drain water were analyzed every 100 or 200 h during the accelerated test with an ion chromatograph (IC, Dionex, DX-120) [5–7].

CO tolerance was also measured periodically without air bleeding every 1000 h. The concentration of CO in the H_2 fuel was changed in the range of 0–100 ppm at a current density of 200 mA cm^{-2}, and the voltage drop was recorded after 2 h from the introduction of CO at each concentration.

2.3. Accelerated degradation of anode catalyst

Using a fresh MEA, the anode catalyst was intentionally deteriorated by potential cycling to investigate the effect of anode deterioration on membrane degradation. The cell temperature was kept at 70 °C. Argon and pure hydrogen were humidified at 67 °C and flowed through the anode and the cathode, respectively, at 150 mL min^{-1} each. The potential of the anode was swept between the rest potential (ca. 0.12 V) and 1.0 V for 10,000 cycles against the cathode (H^+/H_2) using a potentiostat (Solartron, Model 1287). The degree of deterioration was confirmed by cyclic voltammetry between the rest potential and 0.8 V at 10 mV s^{-1}. An accelerated air-bleeding test was then carried out under the same conditions described in the previous section. Prior to the accelerated test, the cell was operated without air bleeding using pure hydrogen and air for 48 h to wash out residual Ru species in the MEA.

2.4. Rotating ring–disk electrode measurements

The effects of Pt–Ru/C catalyst deterioration on oxygen reduction reaction (ORR) were analyzed using the rotating ring–disk electrode (RRDE) technique [15,16]. A commercially available 50 wt.% Pt–Ru (1:1 in atomic ratio) catalysts supported on Ketjen black (Tanaka Kikinzoku Kogyo) was used for the measurements. The RRDE (Nikko Keisoku) consisted of a glassy carbon (GC) disk and a platinum ring sealed in a polytetrafluoroethylene holder. The geometric surface area of the disk electrode was 0.28 cm^2 (6 mm in diameter), and the collection efficiency N determined using a solution of $Fe(CN)^{3-}$ was 0.36 ± 0.02 (N_{th} = 0.38) [17]. The RRDE was polished to a mirror finish with a 0.05 μm alumina suspension (Baikalox) and then cleaned ultrasonically in highly pure water. The Pt–Ru/C

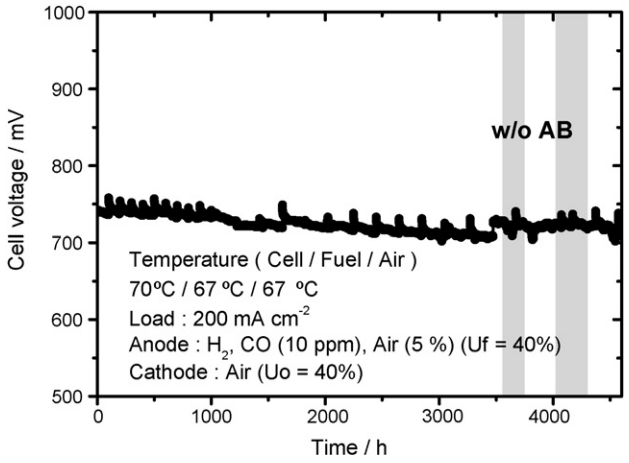

Fig. 1. Variation of cell voltage with time during the accelerated air-bleeding test at 70 °C. H_2 and air were humidified at 67 °C. Fuel: H_2 + 10 ppm CO + 5% air (U_f = 40%); oxidant: air (U_o = 40%), at atmospheric pressure; current density: 200 mA cm^{-2}. Air bleeding was temporarily interrupted in hatched areas.

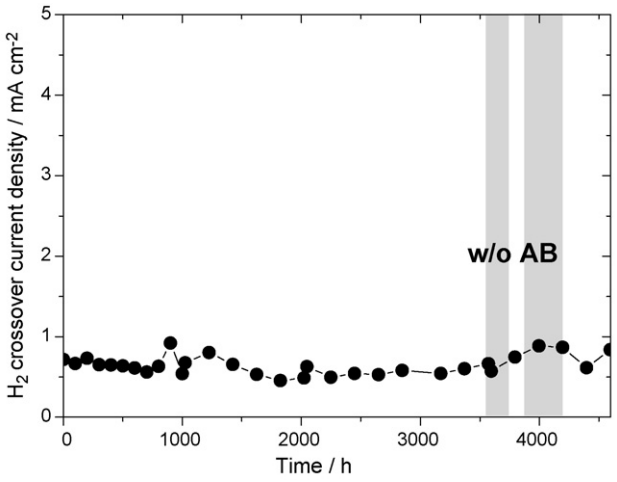

Fig. 2. Variation of H_2 crossover current density with time during the accelerated air-bleeding test in Fig. 1.

catalyst was ultrasonically dispersed in ethanol (Nakalai Tesque) at a concentration of 1 g dm^{-3}. An aliquot of the suspension was carefully dropped on the GC disk electrode with a microsyringe to adjust the metal loading at 56.7 μg_{metal} cm^{-2}, and dried overnight at 60 °C in an electric oven. The catalyst layer on the GC disk was covered with Nafion® coating with a thickness of 0.08 μm from Nafion® solution (Aldrich Chemical Company Inc., 5 wt.%) to fix the catalyst layer on the GC disk [18].

Electrochemical measurements were carried out using a three-electrode glass cell filled with 1.0 M $HClO_4$ solution at 25 °C. The counter and reference electrode was Pt wire and reversible hydrogen electrode (RHE), respectively. The disk potentials were scanned repeatedly for 50,000 cycles between 0.05 and 1.0 V at 1.0 V s^{-1} under argon atmosphere to deteriorate the Pt–Ru/C catalyst. The degree of deterioration was confirmed by cyclic voltammetry between 0.05 and 0.6 V at 50 mV s^{-1}.

Hydrodynamic voltammograms for ORR were measured in O_2-saturated 1.0 M $HClO_4$ solutions at 25 °C using a dual potentiostat (ALS, Model 700A) and a motor speed controller (Nikko Keisoku, RDE-1). The disk and ring electrode was activated separately by repeated potential cycling between 0.05 and 0.6 V and 0.05 and 1.4 V, respectively, at 50 mV s^{-1} under argon atmosphere. After the steady state was attained and the cleanness of the electrodes were confirmed, the disk potential was scanned at 2 mV s^{-1} in the negative-going direction from 1.0 to 0.05 V to obtain oxygen reduction current. The ring potential was kept at 1.2 V, at which H_2O_2 is oxidized to O_2 under diffusion-controlled conditions, to detect H_2O_2 formed at the disk electrode. The rotating rate of the electrode was at 1600 rpm.

3. Results and discussion

3.1. Accelerated air-bleeding test

The variation of cell voltage during the accelerated air-bleeding test is shown in Fig. 1. Periodic voltage changes seen in Fig. 1 are due to electrochemical measurements (i.e., H_2 crossover measurements, etc.). The cell was operated up to 4600 h without a remarkable voltage drop. The average voltage drop rate was about 6 μV h^{-1} up to 4600 h. This value is typical of laboratory test cells, and is about three times higher than that (~2 μV h^{-1}) reported for state-of-the-art MEAs operated under fully humidified conditions [11].

Fig. 2 shows the variation of H_2 crossover current density with time during the accelerated air-bleeding test. The H_2 crossover current density was lower than 1 mA cm^{-2} up to 4600 h, which is a typical value at a cell temperature of 70 °C [5]. The results in Figs. 1 and 2 showed that the membrane was not significantly damaged (i.e., no remarkable membrane thinning and pin-hole formation) up to 4600 h.

On the other hand, fluoride ions were detected from the drain water during the accelerated test. The variation of fluoride-ion release rate (FRR) with time is shown in Fig. 3. The fluoride ions are decomposition products of the PFSA electrolyte membrane [6,8]. FRR was negligibly low up to 2000 h even at 5% air bleeding. The average value of the total FRR (~2000 h)

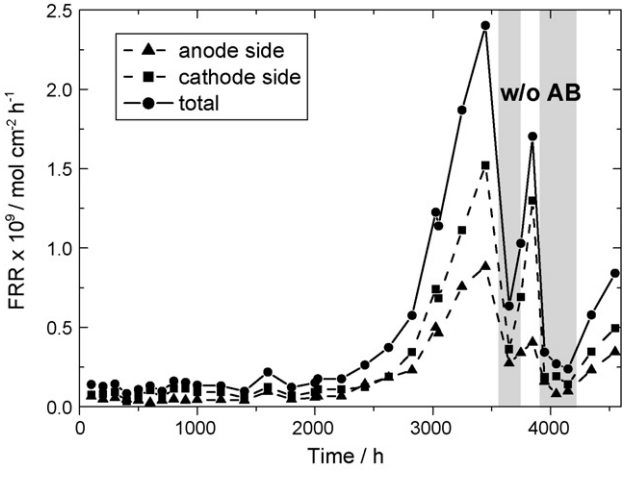

Fig. 3. Variation of fluoride-ion release rate (FRR) in drain water from the anode and the cathode during the accelerated air-bleeding test in Fig. 1.

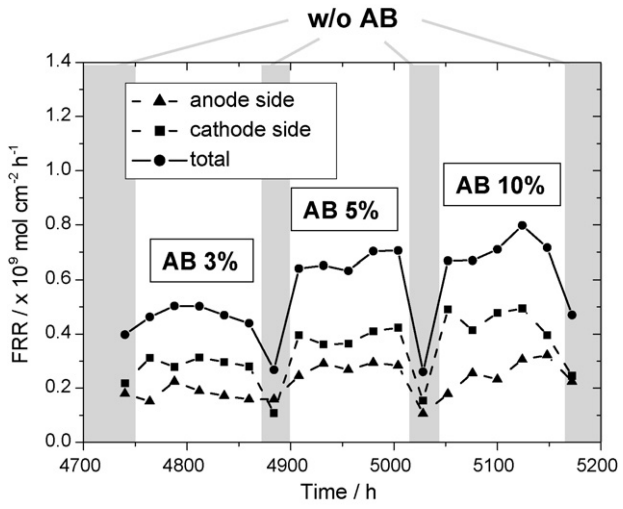

Fig. 4. Changes of fluoride-ion release rate (FRR) with air concentration in the fuel.

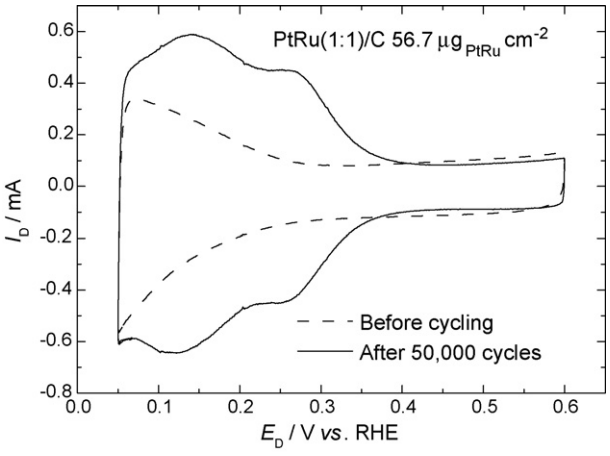

Fig. 6. Cyclic voltammograms at Pt–Ru (1:1)/C catalyst at 50 mV s^{-1} before and after potential cycling in 1.0 M $HClO_4$ under argon atmosphere at 25 °C. Catalyst loading: 56.7 μg_{metal} cm^{-2}; sweep rate: 50 mV s^{-1}. The potential cycling was carried out for 50,000 cycles between 0.05 and 1.0 V at 1.0 V s^{-1}.

was 1.3×10^{-10} mol cm^{-2} h^{-1}, which is two orders of magnitude lower than a typical value of open-circuit durability tests ($\sim 1 \times 10^{-8}$ mol cm^{-2} h^{-1}) [5].

However, FRR gradually increased after 2000 h and reached to 2.4×10^{-9} mol cm^{-2} h^{-1}, the value of which cannot be negligibly low, at 3500 h. When air bleeding was interrupted at around 3600 and 4000 h, FRR dropped significantly, but again increased after air bleeding was re-started.

After 4600 h, the cell was operated without air bleeding for about 100 h to wash out residual H_2O_2, and then air bleeding was re-started to investigate the effect of air concentration. Fig. 4 shows the dependence of FRR on the concentration of air in the fuel. It is clear that FRR increased with increasing air concentration in the fuel. Here FRR dropped again when air bleeding was interrupted. These facts clearly indicated that enhanced membrane degradation after 2000 h was caused by air bleeding.

Fig. 5 shows the variation of CO tolerance of the anode measured during the air-bleeding test in Fig. 1. The CO tolerance of the anode gradually decreased with time. For example, the voltage drop at 100 ppm of CO increased from initial 15 to 22 mV at 4000 h. Though the observed loss of CO tolerance was not so serious, we considered that it is a sign of anode degradation.

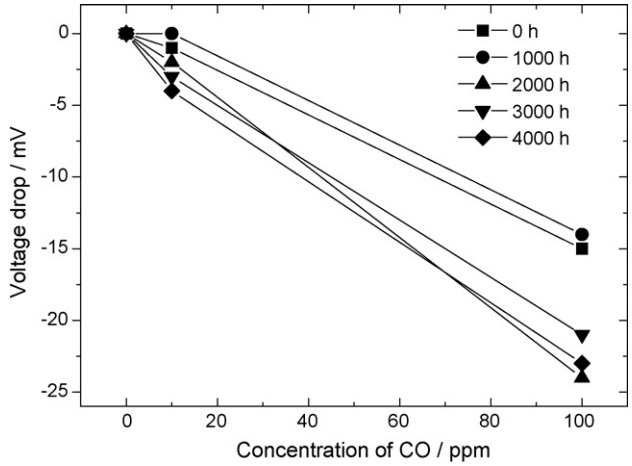

Fig. 5. Changes in CO tolerance during the accelerated air-bleeding test in Fig. 1.

3.2. Effects of Pt–Ru/C catalyst deterioration on ORR

The effects of Pt–Ru(1:1)/C catalyst degradation on ORR were investigated by the RRDE technique. The Pt–Ru(1:1)/C catalyst was dispersed on the GC disk of the RRDE, and was deteriorated by repeated potential cycling for 50,000 cycles between 0.05 and 1.0 V at 1.0 V s^{-1} in 1.0 M $HClO_4$. Fig. 6 shows cyclic voltammograms of in argon atmosphere before and after 50,000 cycles. Fresh Pt–Ru(1:1)/C catalyst showed hydrogen adsorption/desorption peaks typical of Pt–Ru alloy [14,19]. However, two pair of humps appeared at 0.13 and 0.27 V after 50,000 cycles, which indicated that Ru atoms were dissolved and the surface of the catalyst was platinized [20,21].

Hydrodynamic voltammograms in O_2-saturated 1.0 M $HClO_4$ at Pt–Ru(1:1)/C before and after potential cycling are compared in Fig. 7. The disk current (I_D) shows the total current for ORR. The onset of I_D for ORR was shifted to a higher potential after 50,000 cycles, which confirmed that the surface of the catalyst was platinized during potential cycling. The ring current (I_R) is a measure of H_2O_2 formation at the disk electrode. The yield for H_2O_2 formation ($X_{H_2O_2}$) was calculated from the I_D and I_R in Fig. 7 using the following equation [16]:

$$X_{H_2O_2} = \frac{2I_R/N}{I_D + (I_R/N)} \quad (6)$$

The variations of $X_{H_2O_2}$ at Pt–Ru(1:1)/C with the disk potential before and after potential cycling are shown in Fig. 8. Before potential cycling, hydrogen peroxide was formed at potentials more negative than 0.8 V, and the yield increased with a drop in potential. The yield was then levelled off at potentials more negative than 0.4 V, and was only about 4% at 0.05 V. Similar behavior has been reported in the literature [14]. After potential cycling, the H_2O_2 yield decreased in a potential range of

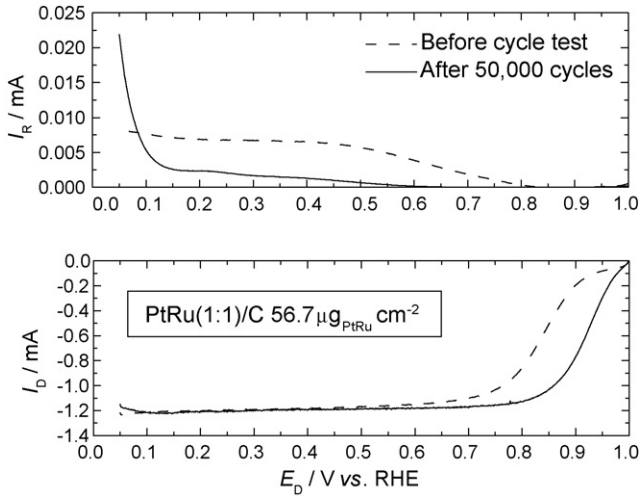

Fig. 7. Hydrodynamic voltammograms for ORR at Pt–Ru (1:1)/C before and after potential cycling in O_2-saturated 1.0 M $HClO_4$ at 25 °C. Catalyst loading: 56.7 μg_{metal} cm^{-2}; sweep rate: 2.0 mV s^{-1}.

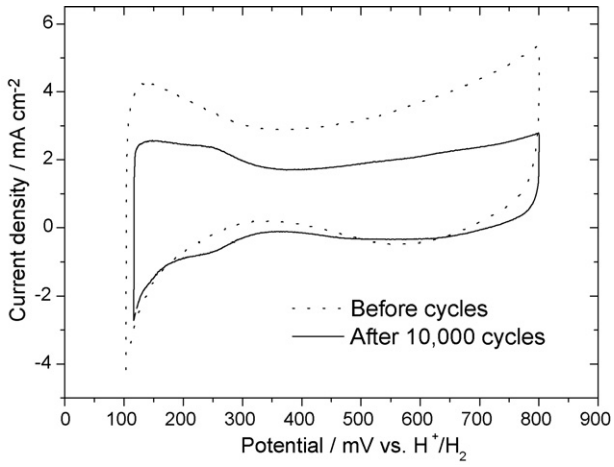

Fig. 9. Cyclic voltammograms at the anode catalyst of a single cell at 10 mV s^{-1} before and after potential cycling. The potential cycling was carried out for 10,000 between the rest potential (0.12 V) and 1.0 V at 100 mV s^{-1}.

0.8–0.2 V. However, it increased significantly with a drop in potential below 0.2 V, and reached 10% at 0.05 V. These features are very similar to those of Pt/C catalyst [14–16], and again due to the surface platinization upon potential cycling. The remarkable increase in H_2O_2 yield below 0.2 V has been attributed to the dissociative adsorption of hydrogen on Pt surface [22]. The observed small H_2O_2 yield at the fresh Pt–Ru(1:1)/C is probably due to much weaker adsorption of hydrogen atoms on the surface. It is therefore concluded that degradation of Pt–Ru/C catalyst enhances H_2O_2 formation upon air bleeding.

3.3. Accelerated degradation of anode catalyst in MEA

The anode catalyst of a fresh MEA was forced to be deteriorated to investigate the effects of anode deterioration on membrane degradation under air-bleeding conditions. After being aged for 100 h, the anode catalyst was deteriorated by potential cycling. Fig. 9 shows cyclic voltammograms of the anode catalyst before and after potential cycling between the rest potential (0.12 V) and 1.0 V at 100 mV s^{-1}. After 10,000 cycles, the shape of the hydrogen adsorption/desorption peaks slightly changed, though the changes were not as remarkable as those observed in Fig. 6. A pair of humps appeared at 0.27 V, which indicated surface platinization of the anode catalyst. The change in CO tolerance of the anode catalyst before and after potential cycling is shown in Fig. 10. The CO tolerance was greatly dropped after potential cycling, which clearly indicated that the anode catalyst was deteriorated during potential cycling.

Fig. 11 shows the variation of FRR before and after potential cycling. Before cycling, FRR was negligibly low even at 5% air bleeding (<1.0×10^{-10} mol cm^{-2} h^{-1}). However, FRR increased with operation time after potential cycling, and reached 3.8×10^{-10} mol cm^{-2} h^{-1} at 300 h after the potential cycling test. It should be noted that the increase in FRR started at around 2000 h without potential cycling as shown in Fig. 3. Hence the observed increase in FRR in Fig. 11 is attributable to the degradation of the anode catalyst by potential cycling.

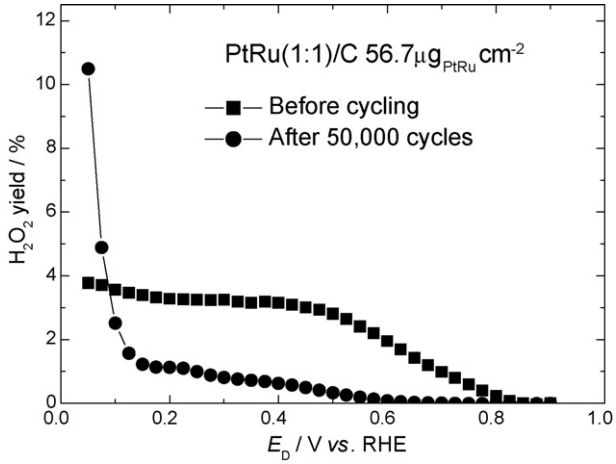

Fig. 8. H_2O_2 yield plotted against the potential at Pt–Ru (1:1)/C catalyst before and after potential cycling. Catalyst loading: 56.7 μg_{metal} cm^{-2}.

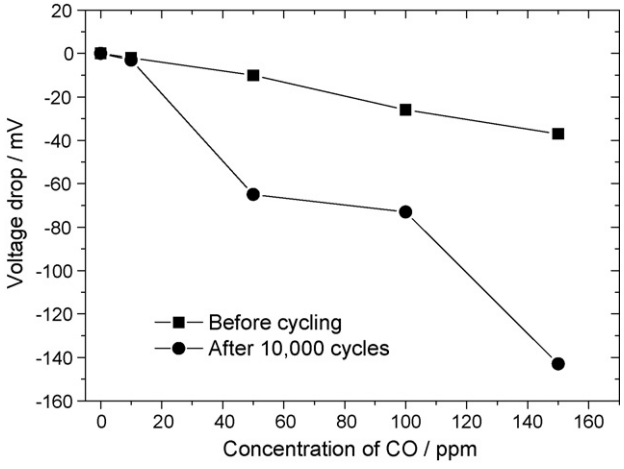

Fig. 10. Changes in CO tolerance of the anode catalyst of a single cell before and after potential cycling (10,000 cycles) between the rest potential (0.12 V) and 1.0 V.

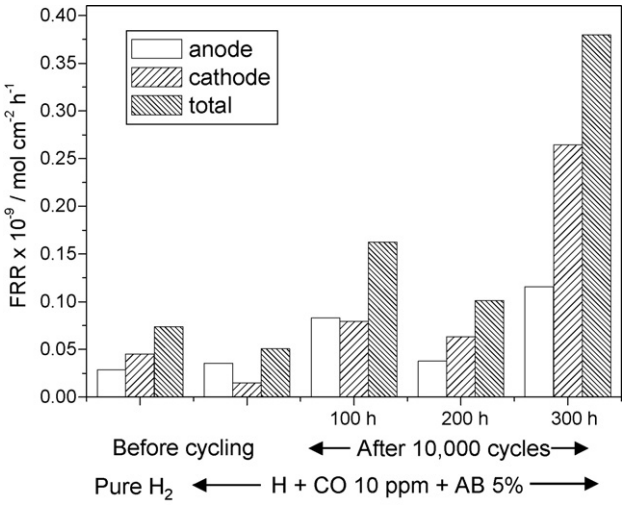

Fig. 11. Variation of fluoride-ion release rate (FRR) in drain water from the anode and the cathode before and after potential cycling.

3.4. Mechanism for membrane degradation in accelerated air-bleeding tests

As shown in Fig. 3, FRR was negligibly low up to 2000 h when an excess amount (5%) of air was added to the fuel. It was considered that a large amount of H_2O_2 might be formed by the introduction of oxygen to the anode as described earlier. However, the results of the RRDE measurements revealed that H_2O_2 formation in ORR at fresh Pt–Ru/C catalyst was relatively low (<4%). In addition, even if H_2O_2 molecules are formed at the anode upon air bleeding, most of them will be further reduced to water when they diffused through the anode catalyst layer to the bulk membrane as

$$H_2O_2 + 2H^+ + 2e^- \rightarrow 2H_2O, \quad E^0 = 1.77\,V \tag{7}$$

Therefore it can be expected that moderate air bleeding (~0.5%) employed under normal operating conditions does not cause serious membrane degradation under highly humidified conditions.

On the other hand, FRR gradually enhanced with time after 2000 h. It increased with air concentration in the fuel, and remarkably dropped when air bleeding was interrupted. Hence the membrane degradation was most probably caused by the formation of H_2O_2 in ORR of the oxygen in the fuel at the anode after 2000 h. The operating time of 2000 h seems to be too long to consider as an induction time for accumulation of H_2O_2 in the membrane. CO tolerance gradually dropped as shown in Fig. 5, which is a sign of anode deterioration, and it is therefore reasonable to consider that the deterioration of Pt–Ru/C anode catalyst is the reason for the enhanced membrane degradation after 2000 h.

The mechanism for the enhanced membrane degradation after 2000 h is considered as follows: excess air bleeding (5%) first deteriorated the anode Pt–Ru/C catalyst. Although the exact reason why the Pt–Ru/C catalyst was deteriorated is not clear at present, it may be due to the heat generated upon catalytic combustion of hydrogen with oxygen in air [12]. The deterioration of the catalyst seems to have proceeded in only a limited part of the MEA, because the drop in CO tolerance was not so serious even at 4000 h as shown in Fig. 5. Hence the deterioration of the catalyst occurs most probably upstream near the inlet, because oxygen molecules would be consumed promptly when contacted with the anode catalyst. Once the Pt–Ru/C catalyst was deteriorated and the surface was platinized, it enhanced H_2O_2 generation as is evidenced by the results in Figs. 7 and 8. Though the H_2O_2 molecules formed at the catalyst were partly reduced to water when they diffused through the catalyst layer at a potential ~0 V, they would not have been completely reduced to water in the catalyst layer. Thus H_2O_2 molecules accumulated in the membrane and produced $^{\bullet}OH$ radicals in the presence of impurity cations such as Fe^{2+}, which resulted in the observed membrane degradation after 2000 h.

4. Conclusions

A long-term accelerated test (4600 h) of a 25 cm^2 single cell with excess air bleeding (5%) was carried out to investigate the effects of air bleeding on membrane degradation in PEFCs. The rate of membrane degradation was negligibly low (FRR = 1.3×10^{-10} mol cm^{-2} h^{-1} in average) up to 2000 h. However, membrane degradation rate was gradually enhanced after 2000 h. The CO tolerance of the anode gradually dropped, which indicated that the anode catalyst was deteriorated during the test. The results of the RRDE measurements revealed that deterioration of Pt–Ru/C catalyst by potential cycling greatly enhances H_2O_2 formation in ORR in the anode potential range (~0 V). In addition, membrane degradation rate of the MEA increased after the anode catalyst was forced to be deteriorated by potential cycling. It was concluded that excess air bleeding deteriorated the anode catalyst, which greatly enhanced H_2O_2 formation upon air bleeding and resulted in the increased membrane degradation rate after 2000 h. The exact reason for the anode-catalyst degradation upon air bleeding is not clear at present, and is now under investigation.

Acknowledgments

This work was supported by Research and Development of Polymer Electrolyte Fuel Cells from New Energy and Industrial Technology Development Organization (NEDO), Japan, and by the Academic Frontier Research Project on "Next Generation Zero-emission Energy Conversion System" of Ministry of Education, Culture, Sports, Science and Technology (MEXT), Japan.

References

[1] A. Pozio, R.F. Silva, M.D. Francesco, L. Giorgi, Electrochim. Acta 48 (2003) 1543.
[2] H. Gasteiger, W. Gu, R. Makharia, M. Mathias, B. Sompalli, in: W. Vielstich, H.A. Gasteiger, A. Lamm (Eds.), Handbook of Fuel Cells, vol. 3, John Wiley & Sons, New York, 2003, pp. 595–596.
[3] Y. Oomori, O. Yamazaki, T. Tabata, Proceedings of the 11th FCDIC Fuel Cell Symposium, FCDIC, Tokyo, 2003, pp. 99–102 (in Japanese).

[4] J. Xie, D.L. Wood, D.M. Wayne, T.A. Zawodinski, P. Atanassov, R.L. Borup, J. Electrochem. Soc. 152 (2005) A104.
[5] M. Inaba, T. Kinumoto, M. Kiriake, R. Umebayashi, A. Tasaka, Z. Ogumi, Electrochim. Acta 51 (2006) 5746.
[6] T. Kinumoto, M. Inaba, Y. Nakayama, K. Ogata, R. Umebayashi, A. Tasaka, Y. Iriyama, T. Abe, Z. Ogumi, J. Power Sources 158 (2006) 1222.
[7] M. Inaba, H. Yamada, R. Umebayashi, M. Sugishita, A. Tasaka, Electrochemistry 75 (2007) 207.
[8] D.E. Curtin, R.D. Lousenberg, T.J. Henry, P.C. Tangeman, M.E. Tisack, J. Power Sources 131 (2004) 41.
[9] M.F. Mathias, R. Makharia, H.A. Gasteiger, J.J. Conley, T.J. Fuller, C.J. Gittleman, S.S. Kocha, D.P. Miller, Interface (2005) 24.
[10] A. Ohma, S. Suga, S. Yamamoto, K. Shinohara, J. Electrochem. Soc. 154 (2007) B757.
[11] Osaka Science and Technology Center, Study on Degradation Factors of PEFCs, PEFC R&D Report, NEDO, Japan, 2006.
[12] M. Inaba, H. Yamada, M. Sugishita, Nenryo Denchi 6 (2007) 16 (in Japanese).
[13] S. Gottesfeld, J. Pafford, J. Electrochem. Soc. 135 (1988) 2651.
[14] V. Stamenkovic, B.N. Grgur, P.N. Ross, N.M. Markovic, J. Electrochem. Soc. 152 (2005) A277.
[15] T.J. Schmidt, H.A. Gasteiger, R.J. Behm, J. Electrochem. Soc. 134 (1998) 2713.
[16] M. Inaba, H. Yamada, J. Tokunaga, A. Tasaka, Electrochem. Solid-State Lett. 7 (2004) A474.
[17] A.J. Bard, L.R. Faulkner, Electrochemical Methods, 2nd ed., Wiley, New York, 2000, p. 331.
[18] E. Higuchi, H. Uchida, M. Watanabe, J. Electroanal. Chem. 583 (2005) 69.
[19] C.L. Green, A. Kucernak, J. Phys. Chem. B 106 (2002) 1036.
[20] H. Yamada, D. Shimoda, K. Matsuzawa, A. Tasaka, M. Inaba, ECS Trans. (2007), in press.
[21] M. Inaba, M. Ando, A. Hatanaka, A. Nomoto, K. Matsuzawa, A. Tasaka, T. Kinumoto, Y. Iriyama, Z. Ogumi, Electrochim. Acta 52 (2006) 1632.
[22] N.M. Markovic, H.A. Gasteiger, P.N. Ross, J. Phys. Chem. 99 (1995) 3411.